

Multi-UAV Collision Avoidance using Multi-Agent Reinforcement Learning with Counterfactual Credit Assignment

Shuangyao Huang, Haibo Zhang and Zhiyi Huang

Abstract—Multi-UAV collision avoidance is a challenging task for UAV swarm applications due to the need of tight cooperation among swarm members for collision-free path planning. Centralized Training with Decentralized Execution (CTDE) in Multi-Agent Reinforcement Learning is a promising method for multi-UAV collision avoidance, in which the key challenge is to effectively learn decentralized policies that can maximize a global reward cooperatively. We propose a new multi-agent critic-actor learning scheme called *MACA* for UAV swarm collision avoidance. *MACA* uses a centralized critic to maximize the discounted global reward that considers both safety and energy efficiency, and an actor per UAV to find decentralized policies to avoid collisions. To solve the credit assignment problem in CTDE, we design a counterfactual baseline that marginalizes both an agent's state and action, enabling to evaluate the importance of an agent in the joint observation-action space. To train and evaluate *MACA*, we design our own simulation environment *MACAEnv* to closely mimic the realistic behaviors of a UAV swarm. Simulation results show that *MACA* achieves more than 16% higher average reward than two state-of-the-art MARL algorithms and reduces failure rate by 90% and response time by over 99% compared to a conventional UAV swarm collision avoidance algorithm in all test scenarios.

I. INTRODUCTION

UAV swarms have become popular in many practical scenarios such as surveillance, transportation, agriculture, search and rescue in hardly-accessible areas and so on. A UAV swarm is a group of UAVs collaborating with each other to accomplish a common mission. Each member in a UAV swarm needs to avoid collisions with not only the obstacles (e.g. birds and adversary UAVs) but also the neighboring swarm members. If each member selects actions independently, more collisions may occur as the action chosen by one member will affect other members. Hence, cooperative path planning is needed for collision avoidance in a UAV swarm, which still remains a critical challenge.

Conventional swarm planning methods suffer from drawbacks including high computational complexity, long reaction time and the need of global environment information to generate collision-free paths. For example, centralized approaches [1], [2] use heuristic algorithms such as A* to select optimal collision-free paths by considering all possible way points in the environment at each planning step. Except the need of knowledge on global environment, the computational complexity grows significantly with the increase on environment size. Decentralized methods such as

E²Coop [3] allows each swarm member to plan its energy-efficient and collision-free trajectories using Particle Swarm Optimization (PSO) combined with Artificial Potential Field (APF), but rely on highly reliable UAV-to-UAV communication for cooperative collision avoidance. Considering the constraints on computing resources and battery lifetime for UAVs as well as the complexity of air traffic, low-complexity collision avoidance methods with short reaction time and high energy-efficiency is more desirable for UAV swarms.

Multi-Agent Reinforcement Learning (MARL) is a promising method for multi-UAV collision avoidance by modeling the problem as a decentralized partially observable Markov decision process (Dec-POMDP), considering UAVs in a swarm as agents in RL. Especially, the Centralized Training with Decentralized Execution (CTDE) paradigm in MARL allows to train multiple agents in a centralized manner using local and global information that cannot be acquired in execution, while in execution, agents make decisions based on only local observations in a decentralized way. This significantly shifts the complexity to training and makes execution extremely lightweight. In order to train multiple agents to achieve the best team performance, it is important to maximize a global reward in the centralized training. However, when agents learn from a global reward independently, the lazy agent problem arises, where a bad action made by one agent may be rewarded due to the good actions performed by others agents. Credit assignment, which attributes the global reward according to the contribution of each agent, is of crucial importance in learning effective decentralized policies. Value factorization based methods such as VDN [4], QMix [5], and QTRAN [6] train a local critic for each agent and factorize the local critic values into a global value. However, this requires to explicitly define the relation between the global and local values, which is nontrivial. Another class of methods such as COMA [7] and Shapley [8] trains a centralized critic for all agents. An advantage function is explicitly derived for each agent to estimate its contribution from the centralized critic using difference rewards. However, COMA is designed for discrete action space. Although it can be extended to continuous action space using Gaussian approximation, the performance is poor when the sampling granularity is low. As a result, the actors fail to learn optimal policies and the trajectories are neither energy efficient nor safe. When the sampling granularity is high, the network structure becomes complex and the computational complexity increases. Shapley also has a high computational complexity since its advantage function is computed over all possible agent combinations.

The authors are with Department of Computer Science, University of Otago, 133 Union Street East, Dunedin 9016, New Zealand {shuangyao, haibo, hzy}@cs.otago.ac.nz

In this paper, we present *MACA*, a Multi-Agent reinforcement learning based scheme with Counterfactual credit Assignment for collision avoidance in UAV swarms. *MACA* consists of a centralized critic network and a local actor network for each swarm member. The critic and actor networks are trained to optimize a global reward that considers both safety and energy efficiency. Unlike COMA, *MACA* is designed for continuous action space and thus need neither sampling nor approximation. Compared with Shapley, its advantage function can be computed by a simple forward pass of the critic with low complexity. To the best of our knowledge, *MACA* is the first to use multi-actor centralised critic reinforcement learning for multi-UAV collision avoidance. The main contributions can be summarized as:

- We formulate the path planning problem for collision avoidance in a UAV swarm as a decentralized partially observable Markov decision process (Dec-POMDP). A new reward function is designed by considering both safety and energy efficiency in collision avoidance.
- We design a multi-actor centralized critic learning scheme for UAV swarm collision avoidance. A new advantage function with low complexity is designed. We theoretically prove the convergence of our learning scheme.
- We also design an emergency avoidance scheme at the control level to complement the actor model to further boost the success rate of collision avoidance.
- We design a MARL environment named *MACAEnv* to train and evaluate *MACA*. Extensive experiments are conducted to demonstrate the effectiveness and efficiency of our scheme.

II. RELATED WORK

A. Collision Avoidance For UAV Swarms

Intensive research has been conducted on collision avoidance for UAV swarms. Conventional methods include Velocity Obstacles (VO) [9], Artificial Potential Field (APF) [10], Particle Swarm Optimization (PSO) [11] and hybrid methods [3]. VO based methods require reliable communications among UAVs. The trajectories planned using VO are usually Zig-Zag, as the UAVs change velocities frequently. Hence, the trajectories are not energy efficient. APF based methods didn't address the problem of coordination among UAVs. Repulsive forces added between UAVs to avoid UAV-to-UAV collisions may generate Zig-Zag trajectories like in VO. Hybrid methods combining APF and PSO require large online response time, as the cost function in PSO is usually complex. Decentralized Model Predictive Control (MPC) has been utilized to solve the problem of UAVs collision avoidance [12]. However, MPC follows a leader-follower structure and highly depends on UAV-to-UAV communications. The whole swarm will be in danger if the leader dies or the communication network is interfered.

Independent reinforcement learning has been proposed to better solve the problem of collision avoidance for UAV swarms. Fully decentralized algorithms [13], [14], [15] suffer

non-stationary problems and require UAV-to-UAV or UAV-to-ground communications. Therefore, CTDE based algorithms were designed to address the drawbacks of fully centralized algorithms. MADDPG [16] is a well known MARL algorithm based on CTDE with individual reward. However, MADDPG cannot guarantee the best team performance as agents in MADDPG are trained by individual rewards rather than a global reward, and thus it is not suitable to be used for UAV collision avoidance.

B. Credit Assignment in MARL

In order to train agents to maximize a global reward, it is important to solve the credit assignment problem. Existing credit assignment methods in MARL can be divided in two classes: implicit assignment and explicit assignment.

Examples of implicit credit assignment include VDN [4], QMix [5] and QTRAN [6]. VDN solves the problem of credit assignment by implicitly decomposing the central Q value Q_{tot} to local utility Q_i values additively. QMix factorizes the central critic Q_{tot} monotonically with an additional mixer network that decides weights and bias for Q_i . QTRAN trains a state-value network in addition to VDN to generalize the representation of Q_{tot} . These algorithms cover a wide range of representations of Q_{tot} , but they usually have high computational complexity and require large network size.

COMA [7] is a representative of MARL algorithms with explicit credit assignment, built on the idea of difference rewards [17]. COMA instead utilizes a centralized critic network to approximate an advantage function based on a counterfactual baseline, which is acquired by averaging over the Q values of all possible actions of an agent except the taken action. This requires the centralized critic network to have at least $|\mathcal{A}|$ output heads, where \mathcal{A} is the set of discrete actions of an agent. Therefore, the calculation of baseline can only be performed well on discrete action spaces.

Inspired by COMA, a similar idea has been proposed by [8], where an advantage function for an agent is approximated with the Shapley value of game theory, which is a weighted sum of Q values over all possible agent collations including the ego agent. The computational complexity of the Shapley value is $O(N!)$, where N is the number of agents. In comparison with COMA and Shapley, our scheme *MACA* has much simpler network structures and lower computational complexity, and is also applicable to continuous action space.

III. SYSTEM MODEL AND FRAMEWORK

A. System Model

Each UAV is equipped with a Lidar sensor to detect the positions and velocities of obstacles and its neighboring UAVs. For example, Lidar sensors such as SICK LD-MRS [18] have a horizontal aperture angle of 110° , a working range of $150m$ and weights less than $1Kg$.

A GPS sensor is also required for self-localization. We assume large static obstacles such as buildings have been bypassed in off-line mission planning. So we focus on avoiding collisions with small dynamic obstacles such as adversary UAVs and birds. Hence, it's reasonable to model

obstacles as moving points. However, our method can be extended to deal with large obstacles with any shapes by treating them as discrete points along obstacle's boundary.

In most applications of UAV swarms, UAVs fly at a constant speed along a pre-planned path. When obstacles are detected, UAVs take actions cooperatively to avoid collisions. After collision avoidance, UAVs come back to their pre-planned paths to continue the mission. To ensure safety, the distance between swarm members and obstacles should not be smaller than a safeguard distance d^{obs} and the distance between swarm members should not be smaller than a safeguard distance d^{v2v} . Since both safety and energy efficiency are of critical importance for long-haul UAV applications, our optimization goal is to generate paths for swarm members to avoid collisions with high energy efficiency.

B. Framework of MACA

The key idea of MACA is to exploit Multi-Agent Reinforcement Learning (MARL) under the CTDE paradigm to achieve low-complexity and energy-efficient collision avoidance. As illustrated in Fig. 1, the MARL method adopts an actor-critic model with a centralized critic. In the *centralized training* phase, the central critic model is trained to approximate the cumulative global reward that measures both safety and energy efficiency. We design an agent-specific advantage function to approximate the contribution of each agent by marginalizing out both the agent's observation and action while keeping other agents unchanged. Actor models are then trained to learn policies that maximize the corresponding advantage functions. In the *decentralized execution* phase, each member in the swarm chooses the action to avoid collision using its actor model based on only its local observation. Although all swarm members perform collision avoidance in a decentralized way based on only local observations, the actor models are trained to act cooperatively in a centralized way. Hence, the actions selected by the swarm members in execution are still cooperative with each other.

Safety is of critical importance to UAV applications, whereas the actor models centrally trained with global information cannot always guarantee to choose the correct actions to avoid collisions. An Emergency Avoidance Scheme (EAS) is designed to complement the actor models for further boosting safety. If the action selected by the actor is infeasible, EAS will choose a feasible action close to the action selected by the actor model.

IV. CENTRALIZED TRAINING

A. Dec-POMDP Model

The objective of MACA is to generate paths for UAVs in a swarm to cooperatively avoid collisions while minimizing energy consumption. Such a problem can be modeled as a Decentralized Partially Observable Markov Decision Process (Dec-POMDP) defined by a tuple $(\mathcal{S}, \mathcal{O}, \mathcal{A}, \mathcal{R}, \mathcal{P})$:

1) *State space \mathcal{S} and observation space \mathcal{O}* : the state at time t , denoted by $s_t \in \mathcal{S}$, is a true state of the global environment defined by the positions and velocities of all swarm members and the obstacles detected at time t . Due

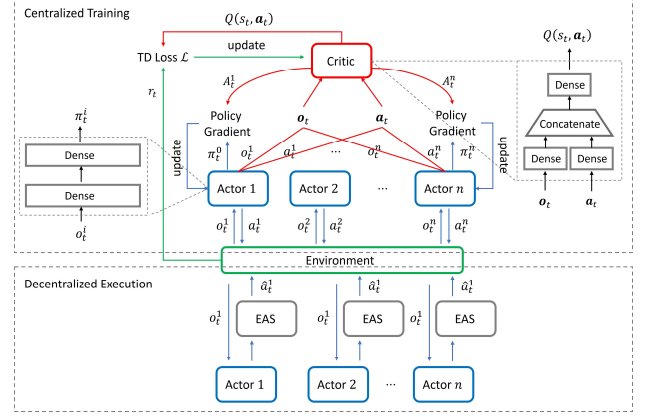


Fig. 1: The framework of MACA.

to limited sensing range, each UAV may only observe a part of the true environment. The observation of the i^{th} UAV at time t , denoted by $o_t^i \in \mathcal{O}$, is represented by an information list that consists of both internal observations and external observations. The internal observations include the UAV's current position, velocity and pre-planned velocity. The external observations include the positions and velocities of other swarm members and obstacles detected by the Lidar sensor. Based on these definitions, we have $s_t \approx o_t = \bigcup_{i=1}^N o_t^i$ where N is the number of UAVs in the swarm.

2) *Action Space \mathcal{A}* : To improve energy efficiency, we confine collision avoidance in a two-dimensional space as altitude flight can consume much more energy than level flight [3]. The control of a UAV can be simplified to the control of Yaw angle when flying with constant speed in an airspace where the air speed can be ignored [3]. However, our scheme can be easily extended to three-dimensional space by setting the control action space to $\{Yaw, Pitch, Roll\}$ angles. In training, we design the action taken by the i^{th} UAV to be $a_i \in [-1, 1]$, corresponding to an Yaw angle change of $[-45^\circ, 45^\circ]$, in order to stabilize training.

3) *Reward Function \mathcal{R}* : To avoid collisions and minimize energy consumption, the reward function is designed to have an internal reward R_t^{Int} that measures energy efficiency and an external reward R_t^{Ext} that reflects safety.

$$R_t = R_t^{Int} + R_t^{Ext},$$

$$R_t^{Int} = \sum_{i=1}^N \left\langle \frac{\mathbf{v}_t^i}{|\mathbf{v}_t^i|}, \frac{\bar{\mathbf{v}}_t^i}{|\bar{\mathbf{v}}_t^i|} \right\rangle - |a_i| - \frac{|\mathbf{x}_t^i, \bar{\mathbf{x}}_t^i|}{D^{max}}, \quad (1)$$

$$R_{Ext} = \begin{cases} 0 & \text{if } Collision = False \\ -C & \text{if } Collision = True \end{cases},$$

where \mathbf{v}_t^i and $\bar{\mathbf{v}}_t^i$ are the current and pre-planned speed of the i^{th} UAV respectively, and $\langle \cdot \rangle$ is inner product. \mathbf{x}_t^i is the current position and $\bar{\mathbf{x}}_t^i$ is the pre-planned position at time t . So, $|\mathbf{x}_t^i, \bar{\mathbf{x}}_t^i|$ measures the distance between the current position and the pre-planned position. D^{max} is an environment specific parameter defining the maximum distance a UAV can deviate from its pre-planned path. The first term in R_t^{Int} guides the UAVs to recover their original

speeds after avoidance. The second term rewards flying along smooth trajectory since the smoother the trajectories the less energy required [3]. The third term aims to drag the UAVs back to their pre-planned paths after avoidance. When either the distance between a UAV and its neighbors falls below the safeguard distance d^{v2v} or the distance between a UAV and an obstacle falls below the safeguard distance d^{obs} , it is assumed collision occurs. In R_{Ext} , C is a model hyperparameter to penalize collisions.

In each training episode, the swarm gets a global reward from the environment as a result of the actions performed by all swarm members. All UAVs in the swarm select actions to maximize the discounted long-term reward $\mathcal{R} = \sum_{l=0}^{\infty} \gamma^l R_{t+l}$, where $\gamma \in [0, 1)$ is a discounted factor.

B. Architecture of multi-actor centralized critic

The centralized critic processes inputs using a dense layer with 64 neurons, of which 32 neurons are used for joint observations and the others are used for joint actions. The observations and actions are concatenated as inputs for two dense layers with 256 neurons followed by ReLU activation functions. Finally, a dense output layer produces $Q(s, \mathbf{a})$. The actor network has a simple architecture consisting of two dense layers with 256 hidden units, followed by ReLU activation functions. Finally, the output layer gives an action a_i using a tanh activation function.

The centralized critic $f^c(s, \mathbf{a}, \omega)$ is trained to approximate the action value function $Q(s, \mathbf{a}) = \mathbb{E}_{s_t, \mathbf{a}_t} [\mathcal{R}_t | s_t, \mathbf{a}_t]$ for the joint action \mathbf{a} and global state s , where $\mathcal{R}_t = \sum_{l=0}^{\infty} \gamma^l r_{t+l}$ is the discounted cumulative reward. Specifically, the critic parameters ω are updated by minibatch gradient descent that minimizes the following loss:

$$\begin{aligned} \mathcal{L}_t^c &= (y_t - f_t^c(s, \mathbf{a}, \omega))^2, \\ y_t &= r_t + \gamma \cdot f_t^c(s, \mathbf{a}, \bar{\omega}), \end{aligned} \quad (2)$$

where $\bar{\omega}$ are parameters of a target network which are periodically updated by ω [19]. The target network has the same structure with the centralized critic, but has its own parameter set. The target network is used to cut bootstrap in calculating \mathcal{L}_t^c to stabilize the training process.

Each actor i is then trained following a policy gradient:

$$g_i = \mathbb{E}_{\pi} [\nabla_{\theta} \log \pi_i(s_i, \theta) A_i(s, \mathbf{a})] \quad (3)$$

where $A_i(s, \mathbf{a})$ is the advantage function for actor i . Unlike COMA and Shapley in which their advantage functions marginalize only the action a_i , our advantage function $A_i(s, \mathbf{a})$ marginalizes both o_i and a_i as follows:

$$A_i(s, \mathbf{a}) = Q(s, \mathbf{a}) - Q(s - o_i, \mathbf{a} - a_i), \quad (4)$$

where $Q(s - o_i, \mathbf{a} - a_i)$ is computed using the critic by replacing both o_i and a_i with `null`, as if actor i observes nothing and takes no action. In COMA and Shapley, the counterfactual baseline is calculated by replacing the action while keeping the others unchanged. This can be seen as evaluating the contribution of an agent's action given the agent's observation in a one dimensional space. While in our

scheme, the counterfactual baseline is calculated by replacing both an actor's observation and action. This can be seen as evaluating the importance of an agent (an observation-action pair) in a two dimensional space. In comparison with COMA and Shapley, our advantage function is also much simpler as it can be computed by a single pass of the critic, whereas the time complexity for the advantage function in COMA is $O(|\mathcal{A}|)$ as its baseline is summed over all possible actions of an actor, and the time complexity for the advantage function in Shapley is $O(N!)$ as its baseline is summed over all possible actor combinations.

Lemma 1: If the global Q-value is a linear combination of all individual contributions, $A_i(s, \mathbf{a})$ is the contribution made by actor i at state s with action a_i when the centralized critic converges to represent the global Q-value function.

Proof: We use $Q_i(s, o_i, a_i)$ to denote the utility value of actor i with state s , observation o_i and action a_i . Note that it is called the utility value rather than Q value because this value does not follow Bellman equation. Let $m(\cdot)$ be the function mapping Q values of individual actors to the global Q value, that is,

$$Q(s, \mathbf{a}) \rightarrow m(Q_0(s, o_0, a_0), Q_1(s, o_1, a_1), \dots, Q_N(s, o_N, a_N))$$

Since the global Q-value is a linear combination of all individual contributions, we have

$$Q(s, \mathbf{a}) = \sum_{i=1}^N Q_i(s, o_i, a_i). \quad (5)$$

Based on the advantage function defined in Eq. (4),

$$\begin{aligned} A_i(s, \mathbf{a}) &= Q(s, \mathbf{a}) - Q(s - o_i, \mathbf{a} - a_i) \\ &= m(\dots, Q_{i-1}, Q_i, Q_{i+1}, \dots) - m(\dots, Q_{i-1}, Q_{i+1}, \dots) \\ &= \sum_{j=1}^N Q_j(s, o_j, a_j) - \sum_{j=1}^{i-1} Q_j(s, o_j, a_j) - \sum_{j=i+1}^N Q_j(s, o_j, a_j) \\ &= Q_i(s, o_i, a_i) \end{aligned}$$

■

According to the reward function defined in Eq. (1), the global reward is a linear combination of all local rewards. In the following lemma, we show that the baseline used in Eq. (4) does not affect the convergence of the centralized critic.

Lemma 2: For a critic following our policy gradient at step t :

$$\begin{aligned} g_t &= \mathbb{E}_{\pi} \left[\sum_i \nabla_{\theta} \log \pi_i(s_i, \theta) A_i(s, \mathbf{a}) \right], \\ A_i(s, \mathbf{a}) &= Q(s, \mathbf{a}) - Q(s - o_i, \mathbf{a} - a_i), \end{aligned} \quad (6)$$

the state-action dependent baseline $Q(s - o_i, \mathbf{a} - a_i)$ doesn't introduce any bias to the critic, and hence does not affect the convergence of the policy gradient algorithm.

Proof: Let $\pi(s)$ be the joint policy which is a product of the policy for all actors as follows: $\pi(s) = \prod_i \pi_i(s_i)$. Then the proof for this lemma can follow the same logic for the convergence proof of single agent actor-critic algorithm [20]. Let $d^{\pi}(s)$ be the discounted state distribution defined

as follows: $d^\pi(s) = \sum_{t=0}^{\infty} \gamma^t Pr(s_t = s | s_0, \pi)$ [20]. Then the expectation on baseline is:

$$\begin{aligned}
g_b &= -\mathbb{E}_\pi \left[\sum_i \nabla_\theta \log \pi_i(s_i, a_i) Q(s - o_i, \mathbf{a} - a_i) \right] \\
&= -\sum_s d^\pi(s) \sum_i \sum_{s^{-i}} \sum_{\mathbf{a}^{-i}} \pi(s - o_i, \mathbf{a} - a_i) \cdot \\
&\quad \sum_{s^i} \sum_{a^i} \pi_i(s_i, a_i) \nabla_\theta \log \pi_i(s_i, a_i) Q(s - o_i, \mathbf{a} - a_i) \\
&= -\sum_s d^\pi(s) \sum_i \sum_{s^{-i}} \sum_{\mathbf{a}^{-i}} \pi(s - o_i, \mathbf{a} - a_i) \cdot \\
&\quad \sum_{s^i} \sum_{a^i} \nabla_\theta \pi_i(s_i, a_i) Q(s - o_i, \mathbf{a} - a_i) \\
&= -\sum_s d^\pi(s) \sum_i \sum_{s^{-i}} \sum_{\mathbf{a}^{-i}} \pi(s^{-i}, \mathbf{a}^{-i}) Q(s - o_i, \mathbf{a} - a_i) \nabla_\theta 1 \\
&= 0.
\end{aligned}$$

As shown above, the baseline doesn't introduce bias although it is state-action dependent. Hence, the baseline doesn't affect the convergence of the algorithm. ■

V. DECENTRALIZED EXECUTION

Only actor models are used in execution. Actor i takes only its local observation o_i as input and outputs the optimal action a_i . However, since actor models have a certain failure rate, an Emergency Avoidance Scheme (EAS) is needed at the control level during online execution to complement the actor models to make up for the failure rate.

Let $d_i^{obs}(a_i)$ and $d_i^{v2v}(a_i)$ be the distances from UAV i to any obstacle and any neighbor at the beginning of the next control loop respectively if the UAV takes action a_i in the current control loop. Since each UAV knows its current position, action and neighboring environments, $d_i^{obs}(a_i)$ and $d_i^{v2v}(a_i)$ are easy to predict. A policy action is infeasible if

$$d_i^{obs}(a_i) \leq d^{obs} \text{ or } d_i^{v2v}(a_i) \leq d^{v2v}, \quad (7)$$

where d^{obs} and d^{v2v} are the safeguard distances to obstacles and neighbors, respectively.

If the action selected the actor model is infeasible, a set of candidate actions are generated without duplicates with a Gaussian noise centered on the policy action:

$$\tilde{\mathcal{A}}_i \sim \mathcal{N}(a_i, \sigma_{exe}). \quad (8)$$

The infeasible actions are first excluded from $\tilde{\mathcal{A}}_i$ based on Eq. (7). The final avoiding action \tilde{a}_i is then selected as the nearest candidate to a_i in $\tilde{\mathcal{A}}_i$.

VI. PERFORMANCE EVALUATION

We first present the simulation environment designed to train MACA and then discuss the testing results in comparison with other algorithms. The code for MACA and MACAEnv are available at <https://github.com/OtagoCSSystemsGroup/MACA>.

A. Simulation environment - MACAEnv

Existing MARL environments such as StarCraft II [21], Multiple Particle Environment [22] or Multi-Robot Warehouse [23] cannot closely mimic the multi-UAV applications. A new multi-agent environment, *MACAEnv*, is developed to evaluate the performance of our algorithm and other algorithms. *MACAEnv* is an episodic environment. An episode starts when a swarm of UAVs and obstacles are spawned and ends when either collision occurs or the obstacles fly through the screen without collisions. For each step in an episode, all UAVs take actions synchronously.

The environment is shown in Fig. 2. The screen is a $300m \times 300m$ square. At any time, a UAV can only observe a circle window with radius $d = 50m$ around itself. So, our agents are quite short sighted to make sure the environment is partially observed. When an episode is initialized, a swarm with N UAVs is spawned around the middle left of the screen. The positions of UAVs \mathbf{x}_s are equally spaced on a circle with radius of r . The setting of r should match with N , such that the distances between any two UAVs are larger than d^{v2v} initially. For example, we set $r = 30m$ for $N = 3$ and $r = 50m$ for $N = 4$. The initial paths of UAVs are horizontal lines starting from their initial positions pointing to the right most of the screen. The initial speed for each UAV is set to $5m/s$. At the same time, M obstacles are spawned around the middle right, top or bottom side of the screen and are set to fly along straight lines pointing toward the swarm with a velocity of $5m/s$. The initial distance between any UAV and any obstacle is larger than $d = 50m$ so that all obstacles are out of the observation window of each UAV initially. In each training step, a Gaussian noise $\mathcal{N}(0, 0.1)$ is added to the selected action with probability ϵ , where ϵ is annealed from 1.0 to 0.1 in $50k$ training steps to encourage UAVs to explore better actions and avoid local optima.

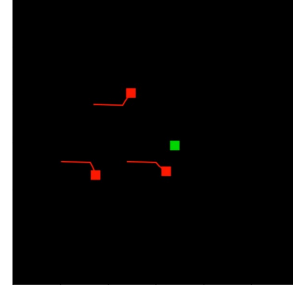


Fig. 2: Snapshots of *MACAEnv* where red and green squares represent UAVs and obstacles, respectively. The red curves represent trajectories of UAVs.

B. Learning Performance

We compare MACA with two state-of-the-art algorithms: COMA [7] and Shapley [8].

- **COMA** computes a counterfactual baseline by marginalizing out an agent's action and averaging over all possible actions in the discrete action space. To compare with COMA in our continuous actions

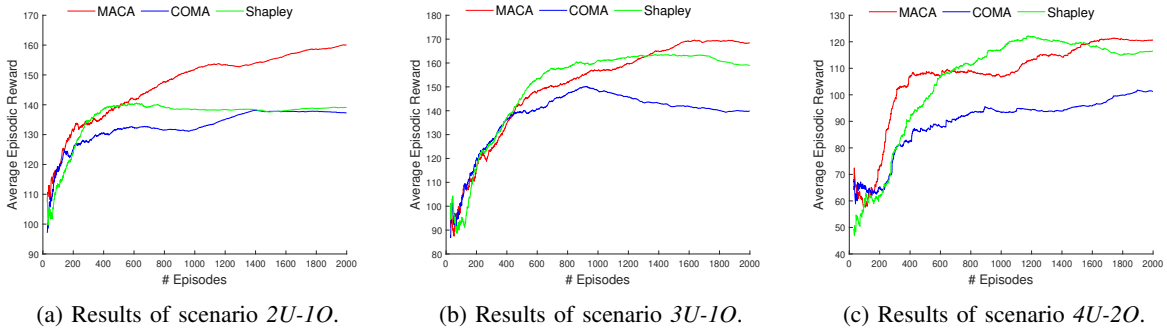


Fig. 3: Learning performance of all three algorithms and parameter analysis of MACA.

space, we add a Gaussian noise to agents' actions. So, a'_i in the advantage function in COMA becomes $a'_i \sim \mathcal{N}(a_i, \sigma)$, where $\sigma = 0.1$.

- **Shapley** computes a baseline for each agent by averaging over all possible collations that include this agent. Its complexity grows with the increase of swarm size.

We perform tests in three scenarios: 2-UAV-1-Obstacle (2U1O), 3-UAV-1-Obstacle (3U1O) and 4-UAV-2-Obstacle (4U2O). We choose small-size swarms in our experiments because the training takes very long time. For example, it takes more than 10 hours to train in any of our scenarios. For larger-size swarms it would take weeks to train. We will provide results for larger swarms in the final version, though the results on small sizes have already validated our theoretical analysis.

In the following experiments, we set $C = 0$ and $D^{max} = 150$ in the reward function for MACA, $\sigma_{exe} = 1.0$ for EAS. The collision penalty C can be set to 0 in *MACAEnv*, because the episode ends once collision occurs. The action causing collision is penalized by ending of game. The test results are shown in Fig. 3. In all scenarios, our scheme achieves the highest reward, COMA achieves the lowest and Shapley ranks in the middle. This is because our scheme doesn't need to select any default action when calculating the counterfactual baseline. The contribution of each agent is purely calculated by the collection of observations and actions from all agents except that agent, which just depends on the current state of the environment. However, the counterfactual baseline in COMA is calculated by averaging over all possible actions in the agent's action space. This counterfactual baseline is representative enough in discrete action spaces where one can loop over all possible actions to calculate the corresponding Q values. But it is not representative enough in continuous action space where the action space is sampled based on a distribution model. In Shapley, the counterfactual baseline is calculated by replacing an agent's action with a default action and then averaging over all possible collations that include the agent per se. When the number of agents is small like three or four, the counterfactual baseline in Shapley is not representative enough and the performance is poor. Fig. 3 also shows that the highest rewards all algorithms can achieve in scenario 4U2O are much lower than those in scenario 2U1O and 3U1O. That is because

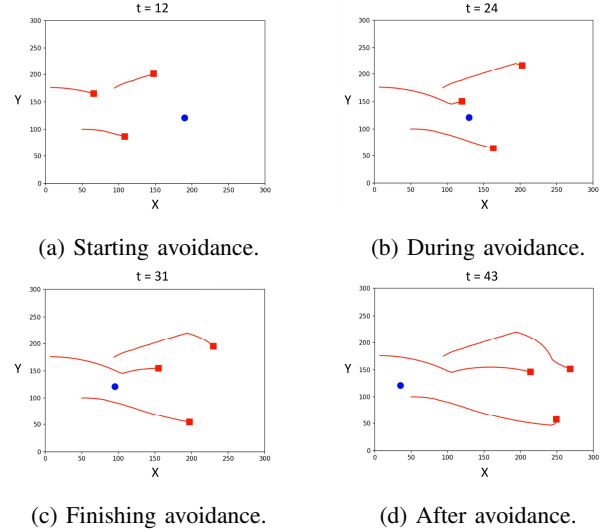


Fig. 4: Demonstrations of trajectories generated by MACA.

the environment is much more complex in scenario 4U2O and its joint action space is also much larger, making it difficult to find the optimal joint actions to achieve high global reward. Overall, our algorithm achieves an average reward that is better (16.61%, 20.41% and 19.22% higher) than the other two algorithms in scenario 2U1O, 3U1O and 4U2O, respectively.

C. Trajectory Demonstration

Fig. 4 shows the trajectories generated by MACA with three UAVs and one obstacle. The UAVs and obstacles all have a velocity of $5m/s$, flying towards each other. The red squares and blue dots represent UAVs and obstacles, respectively. The red curves represent trajectories of UAVs. A short video is also attached with in the submission of this paper to demonstrate the movement and trajectories of UAVs.

D. Safety, Energy and Response time

In this experiment, we compare the safety, energy consumption and response time of MACA, COMA and Shapley against a state-of-the-art conventional algorithm E^2Coop [3]. *Safety* is evaluated by the minimum distance among

	2U1O				3U1O				4U2O			
	Safety (m) d^{obs}, d^{v2v}	Failure rate	Energy ($\times 10^3$ J)	Respond time (s)	Safety (m) d^{obs}, d^{v2v}	Failure rate	Energy ($\times 10^3$ J)	Respond time (s)	Safety (m) d^{obs}, d^{v2v}	Failure rate	Energy ($\times 10^3$ J)	Respond time (s)
E^2Coop	34.52 \pm 0.18, 39.93 \pm 0.18	0%	1.2974	0.3673	24.06 \pm 0.12, 29.20 \pm 0.02	0%	1.2950	0.4666	21.07 \pm 4.01, 24.18 \pm 1.82	21%	1.4245	0.6272
Shapley	47.59 \pm 20.72 94.99 \pm 13.16	3%	2.6661	0.0065	35.33 \pm 10.48 55.42 \pm 11.84	7%	3.0013	0.0070	59.82 \pm 44.27 51.94 \pm 9.71	7%	2.2731	0.0091
COMA	59.19 \pm 24.16 99.83 \pm 1.03	0	2.5680	0.0068	59.19 \pm 24.16 99.83 \pm 1.03	0	2.5680	0.0068	25.40 \pm 2.54, 44.89 \pm 3.63	14%	3.9619	0.0063
MACA(no E)	54.67 \pm 30.86, 97.56 \pm 8.02	0	1.5658	0.0071	44.14 \pm 16.32, 63.16 \pm 14.37	2%	3.0953	0.0090	69.37 \pm 27.71, 42.51 \pm 1.91	12%	2.9142	0.0093
MACA	70.25 \pm 35.06, 97.67 \pm 6.35	0	1.6050	0.0034	44.16 \pm 21.30, 81.58 \pm 9.74	0	2.0437	0.0032	38.09 \pm 20.21, 43.46 \pm 2.51	2%	2.6912	0.0071

Fig. 5: Comparison of MACA with state-of-the-art MARL algorithms and conventional algorithms.

swarm members and the minimum distance between a UAV and an obstacle during avoidance. *Energy consumption* is calculated using the energy model proposed in E^2Coop . For a fair comparison, the power consumption of E^2Coop also includes the energy spent on communication since it highly relies on the vehicle-to-vehicle communication. We assume each UAV uses a WIFI transceiver and the communication power is set to 2W according to the off-the-shelf WIFI radio chips [24]. The weight of a UAV is set to 1Kg. d^{obs} and d^{v2v} are set to 20m and 5m, respectively. We compare our algorithm against E^2Coop under the setting $\theta = 45^\circ$, as it is empirically recommended by our simulations. We also did ablation tests to validate the importance of EAS in decentralized execution. The results are shown in Fig. 5 and all schemes are performed 100 episodes.

It can be seen from Fig. 5 that all MARL algorithms greatly reduce the respond time and achieve lower failure rate compared to E^2Coop . The energy consumption of the three MARL algorithms are slightly higher than E^2Coop . This is because the cost function in E^2Coop penalizes UAVs for deviating from the trajectories that are centrally planned, whereas in MARL algorithms there is no central planning and all trajectories are searched individually with safety being the highest priority. Therefore, UAVs in MARL algorithms try to maintain a relative large distance to neighbors and obstacles. While each UAV in E^2Coop tends to keep a distance close to the safeguard distances while ensuring safety. This also explains why the distances between UAVs and obstacles are generally larger in MARL algorithms than in E^2Coop . Comparing with MACA(noEAS) and the two other MARL algorithms, MACA(noEAS) generally achieves a lower failure rate and consumes less energy. This shows that the counterfactual baseline in our algorithm better represents the importance of each agent, and therefore the agents in our algorithm learn more robust policies.

The biggest advantage of MACA is its short response time for each step. The solutions are found almost instantly by a simple forward pass of the actor models. While in E^2Coop , the solutions are found by repeatedly performing the whole algorithm at each step, considering neighboring UAVs and obstacles. So the respond time of E^2Coop is much larger than that of MACA and grows with the increase on the number of UAVs. MACA(noEAS) also has a failure rate of

2% and 12% in scenario 3U1O and 4U2O, respectively. But with EAS, the failure rate is reduced to 0 and 2% in scenario 3U1O and 4U2O, respectively. Overall, our algorithm reduces respond time by over 99% compared to E^2Coop in all scenarios. We reduce the failure rate by 90% in scenario 4U2O, respectively, even though the energy consumption of MACA increases a little.

VII. CONCLUSION

In this paper, a new multi-actor centralized critic learning scheme named MACA is proposed for collision avoidance of UAV swarms. A new counterfactual advantage function with low complexity is proposed and this advantage function can also apply to continuous action spaces. An emergency avoidance scheme is proposed to accommodate the failure rate of the actor models in execution phase. Comprehensive experiments are conducted in our environment MACAEnv to show the advantage of our algorithm. Future work will focus on further reduction of energy consumption in MACA.

REFERENCES

- [1] K. Jose and D. K. Pratihari, "Task allocation and collision-free path planning of centralized multi-robots system for industrial plant inspection using heuristic methods," *Robotics and Autonomous Systems*, vol. 80, pp. 34–42, 2016. [Online]. Available: <https://www.sciencedirect.com/science/article/pii/S0921889016000282>
- [2] C. Liang, X. Zhang, Y. Watanabe, and Y. Deng, "Autonomous collision avoidance of unmanned surface vehicles based on improved a star and minimum course alteration algorithms," *Applied Ocean Research*, vol. 113, p. 102755, 2021.
- [3] S. Huang, H. Zhang, and Z. Huang, "E2coop: Energy efficient and cooperative obstacle detection and avoidance for uav swarms," in *Proceedings of the International Conference on Automated Planning and Scheduling*, vol. 31, 2021, pp. 634–642.
- [4] P. Sunehag, G. Lever, A. Grusl, W. M. Czarnecki, V. Zambaldi, M. Jaderberg, M. Lanctot, N. Sonnerat, J. Z. Leibo, K. Tuyls *et al.*, "Value-decomposition networks for cooperative multi-agent learning," *arXiv preprint arXiv:1706.05296*, 2017.
- [5] T. Rashid, M. Samvelyan, C. S. de Witt, G. Farquhar, J. Foerster, and S. Whiteson, "Qmix: Monotonic value function factorisation for deep multi-agent reinforcement learning," 2018.
- [6] K. Son, D. Kim, W. J. Kang, D. E. Hostallero, and Y. Yi, "Qtran: Learning to factorize with transformation for cooperative multi-agent reinforcement learning," 2019.
- [7] J. Foerster, G. Farquhar, T. Afouras, N. Nardelli, and S. Whiteson, "Counterfactual multi-agent policy gradients," in *Proceedings of the AAAI Conference on Artificial Intelligence*, vol. 32, no. 1, 2018.

- [8] J. Li, K. Kuang, B. Wang, F. Liu, L. Chen, F. Wu, and J. Xiao, "Shapley counterfactual credits for multi-agent reinforcement learning," *Proceedings of the 27th ACM SIGKDD Conference on Knowledge Discovery and Data Mining*, Aug 2021. [Online]. Available: <http://dx.doi.org/10.1145/3447548.3467420>
- [9] J. Snape, J. Van Den Berg, S. J. Guy, and D. Manocha, "The hybrid reciprocal velocity obstacle," *IEEE Transactions on Robotics*, vol. 27, no. 4, pp. 696–706, 2011.
- [10] S. Huang and K. Low, "A path planning algorithm for smooth trajectories of unmanned aerial vehicles via potential fields," in *2018 15th International Conference on Control, Automation, Robotics and Vision (ICARCV)*. IEEE, 2018, pp. 1677–1684.
- [11] B. Song, Z. Wang, L. Zou, L. Xu, and F. E. Alsaadi, "A new approach to smooth global path planning of mobile robots with kinematic constraints," *International Journal of Machine Learning and Cybernetics*, vol. 10, no. 1, pp. 107–119, 2019.
- [12] Y. Kuriki and T. Namerikawa, "Formation control with collision avoidance for a multi-uav system using decentralized mpc and consensus-based control," *SICE Journal of Control, Measurement, and System Integration*, vol. 8, no. 4, pp. 285–294, 2015.
- [13] D. Wang, T. Fan, T. Han, and J. Pan, "A two-stage reinforcement learning approach for multi-uav collision avoidance under imperfect sensing," *IEEE Robotics and Automation Letters*, vol. 5, no. 2, pp. 3098–3105, 2020.
- [14] Y.-H. Hsu and R.-H. Gau, "Reinforcement learning-based collision avoidance and optimal trajectory planning in uav communication networks," *IEEE Transactions on Mobile Computing*, 2020.
- [15] Y. F. Chen, M. Liu, M. Everett, and J. P. How, "Decentralized non-communicating multiagent collision avoidance with deep reinforcement learning," in *2017 IEEE international conference on robotics and automation (ICRA)*. IEEE, 2017, pp. 285–292.
- [16] R. Lowe, Y. Wu, A. Tamar, J. Harb, P. Abbeel, and I. Mordatch, "Multi-agent actor-critic for mixed cooperative-competitive environments," *arXiv preprint arXiv:1706.02275*, 2017.
- [17] D. H. Wolpert and K. Tumer, "Optimal payoff functions for members of collectives," in *Modeling complexity in economic and social systems*. World Scientific, 2002, pp. 355–369.
- [18] SICK, "Ld-mrs420201," <https://www.sick.com/de/en/detection-and-ranging-solutions/3d-lidar-sensors/ld-mrs/c/g91913>, 2021, (Accessed on 12/16/2021).
- [19] V. Mnih, K. Kavukcuoglu, D. Silver, A. A. Rusu, J. Veness, M. G. Bellemare, A. Graves, M. Riedmiller, A. K. Fidjeland, G. Ostrovski *et al.*, "Human-level control through deep reinforcement learning," *nature*, vol. 518, no. 7540, pp. 529–533, 2015.
- [20] R. S. Sutton, D. A. McAllester, S. P. Singh, and Y. Mansour, "Policy gradient methods for reinforcement learning with function approximation," in *Advances in neural information processing systems*, 2000, pp. 1057–1063.
- [21] O. Vinyals, T. Ewalds, S. Bartunov, P. Georgiev, A. S. Vezhnevets, M. Yeo, A. Makhzani, H. Küttler, J. Agapiou, J. Schrittwieser *et al.*, "Starcraft ii: A new challenge for reinforcement learning," *arXiv preprint arXiv:1708.04782*, 2017.
- [22] R. Lowe, Y. Wu, A. Tamar, J. Harb, P. Abbeel, and I. Mordatch, "Multi-agent actor-critic for mixed cooperative-competitive environments," *arXiv preprint arXiv:1706.02275*, 2017.
- [23] G. Papoudakis, F. Christianos, L. Schäfer, and S. V. Albrecht, "Benchmarking multi-agent deep reinforcement learning algorithms in cooperative tasks," in *Proceedings of the Neural Information Processing Systems Track on Datasets and Benchmarks (NeurIPS)*, 2021. [Online]. Available: <http://arxiv.org/abs/2006.07869>
- [24] D. Halperin, B. Greenstein, A. Sheth, and D. Wetherall, "Demystifying 802.11 n power consumption," in *Proceedings of the 2010 international conference on Power aware computing and systems*. USENIX Association, 2010, p. 1.